minerals

MDPI

Article

Origin and Heavy Metals of Plagio-Granites in Egyptian Shield Oceanic Complexes: A Case Study of Abu Dabbab Area, Central Eastern Desert, Egypt

Hatem M. El-Desoky [1], Ahmed M. Abdel-Rahman [1], Antoaneta Ene [2,*], Ahmed E. Khalil [3], Wael Fahmy [1], Hesham M. H. Zakaly [4,5,*] and Hamdy A. Awad [6,*]

1 Geology Department, Faculty of Science, Al-Azhar University, Cairo 11884, Egypt
2 Department of Chemistry, Physics and Environment, Faculty of Sciences and Environment, INPOLDE Research Center, Dunarea de Jos University of Galati, 47 Domneasca Street, 800008 Galati, Romania
3 Department of Geology, National Research Center, Cairo 12622, Egypt
4 Institute of physics and technology, Ural Federal University, Yekaterinburg 620002, Russia
5 Physics Department, Faculty of Science, Al-Azhar University, Assiut 71524, Egypt
6 Geology Department, Faculty of Science, Al-Azhar University, Assiut 71524, Egypt
* Correspondence: antoaneta.ene@ugal.ro (A.E.); h.m.zakaly@azhar.edu.eg (H.M.H.Z.); hamdiawaad@gmail.com (H.A.A.)

Abstract: Several outcrops of felsic melt, commonly known as oceanic plagio-granites, appear as melt pockets, irregular bosses, and dikes. Three main rock successions were exposed in the Abu Dabbab area: ophiolitic sequence, island arc assemblage, and rare metal-bearing albite granites. Plagio-granite is composed mainly of plagioclase and quartz, and chemically contains high SiO_2, Al_2O_3, and Na_2O values. The petrogenetic and geochemical studies concluded that the magmas of plagio-granites and associated felsic rocks were derived from partial melting of highly depleted mantle harzburgite and/or pre-existing oceanic crustal rocks (basalts and/or gabbros). The geochemical characteristics reveal that Abu Dabbab plagio-granites are identical to the typically low-K series of ophiolitic complexes and resemble the ocean ridge granites. Elements such as Co, Nb, Pb, and Nd in Abu Dabbab plagio-granites have high Clarke concentrations (more than 1.88). This indicates Abu Dabbab plagio-granite derived from partial melting of pre-existing oceanic crustal rocks. The average concentration values of 238 U and 232 Th are lower than those of the world's average and the average activities in granitic rocks. The scope of estimated exercises generally contrasted as their quality in rock tests relies upon their physical, synthetic, and geo-concoction properties and the appropriate condition.

Keywords: plagio-granites; radioactive; Abu Dabbab area; eastern desert; Egypt

check for updates

Citation: El-Desoky, H.M.; Abdel-Rahman, A.M.; Ene, A.; Khalil, A.E.; Fahmy, W.; Zakaly, H.M.H.; Awad, H.A. Origin and Heavy Metals of Plagio-Granites in Egyptian Shield Oceanic Complexes: A Case Study of Abu Dabbab Area, Central Eastern Desert, Egypt. *Minerals* **2022**, *12*, 1093. https://doi.org/10.3390/min12091093

Academic Editor: Federica Zaccarini

Received: 3 August 2022
Accepted: 25 August 2022
Published: 29 August 2022

1. Introduction

The term "oceanic plagio-granite" was first proposed by [1] and is a synonym for TTG (tonalites, trondhjemites, and granodiorites), diorites, abilities, peraluminous leucogranites, and keratophyric occurring in the oceanic crust or in ophiolites. Plagio-granitic intrusions vary from small felsic veins, variable in size [2] and melt pockets, up to intrusive bodies of several 100 m in diameter [3]. They are chemically characterized by high SiO_2, Na_2O, and CaO and low K_2O and FeOt (Coleman and Donato, 1979; Coleman and Peterman, 1975). In [1], the authors refer to the group of leucogranite rocks associated with ophiolitic complexes as oceanic plagio-granites. These rocks range in composition from albite granite through trondhjemites and tonalites to granodiorites. The generation of plagio-granites in ophiolites is an ongoing matter of debate and in the last couple of decades several different models for their generation have been established. However, the formation of

plagio-granite magmas has been explained by either partial melting of pre-existing mafic rocks [4–6]) or by extensive fractional crystallization of a mafic melt [7,8].

Many authors have suggested that the ophiolitic plagio-granites are the product of differentiation of basaltic magma within the oceanic crust and as such represent the final stages of oceanic crust evolution [9,10]. However, other workers have indicated that oceanic plagio-granites (not necessarily related to an ophiolite) may represent partial melts [2,11,12], thereby implying a more complex set of processes than those expected at a rapidly cooling oceanic ridge. Support for the partial melting hypothesis has recently been provided by [13] who have shown that the low-pressure melting of hydrated oceanic gabbro yields plagio-granite melts.

Detailed research on the formation and evolution of plagio-granites has shown that different types of plagio-granites may form during different stages of the evolution of the oceanic crust, from mid-ocean ridge spreading through the migration, subduction, to obduction stages [14–16]. Four genetic types of plagio-granites have been recognized: fractionation-, shearing-, subduction-, and obduction-type [17–20].

Arabian Nubian Shield (ANS) plagio-granite is high in the contents of SiO_2 (70%–77%) and low in K_2O (0.04%–1.9%; [21]). These mostly are of trondhjemite and tonalite on a normative Ab-An-Or diagram. The gabbroic rocks are often intruded by mafic dikes, which represent the base of the sheeted dyke complex. Peraluminous SiO_2-rich leucogranites are commonly used for felsic igneous rocks product of the partial melting of continental crustal rocks during the dehydration melting of muscovite-rich metasediments during regional metamorphism, i.e., the S-type granitoid. In addition, they can be the product of the extreme fractional crystallization of granitic series, i.e., the most evolved terms of granitic series [22].

Egyptian plagio-granite has been studied by a group of scientists in several areas such as Wadi Shait- Gabal El-Maiyat, Wadi Ghadir ophiolite, Wadi Allaqi, and El-Shadli plutonic complex [14,23,24]. Ref. [14] studied the gabbro-diorite suite and felsic dykes crosscutting ophiolitic rocks in Wadi Allaqi southernmost Eastern Desert to establish a minimum age for these ophiolites. A plagio-granite from the Onib ophiolite yielded a Pb–Pb evaporation age of 808 ± 14 Ma [14], significantly older than any other Yoshgah ophiolite age.

Recently, ref. [25] believed that the ocean ridge granites represented by ophiolitic plagio-granites outcropping within the Wadi Garf-Atud-Sukari-Ghadier suture-shear zone and the Um Khariga-Abu Dabbab suture-shear zone. The study of plagio-granite petrogenesis thus provides an opportunity to examine evolutionary processes pertaining to both continental and oceanic crusts. Knowledge of the processes whereby silicic melts are generated from mafic crust helps to understand the genesis of the continental crust [7]. The major problem is interpreting any of the natural plagio-granites as products of silicate liquid immiscibility in the fact that neither the Fe-enriched conjugate liquid nor its crystalline equivalent has been described in the ophiolite or MOR literature. The present work aims to discuss the petrography, geochemistry, and petrogenesis of Abu Dabbab ophiolitic plagio-granites.

The natural radioactivity of rocks is represented by U, Th, and K^{40} (K^{40} represents 0.0118% of total potassium). Natural uranium mainly includes three isotopes: U^{238}, U^{235} and U^{234}. U^{238} represents 99.3%, U^{235} is 0.7% while U^{234} is found in a minute quantity. Both U^{238} and U^{235} decay through a series of short-lived radioactive isotopes to end with stable isotopes of lead (Pb^{206} from U^{238} and Pb^{207} from U^{235}). Radioactive elements (U, Th, and K) are amongst the most incompatible elements, and they are concentrated in granitic rocks. U content mainly increases with SiO_2 content during differentiation, fractional crystallization, partial melting, etc., in the final stage of the magmatic procedures [26,27]. Mostly, the increase in U due to the increase in both SiO_2 and alkali content is usually more marked than the increase in Th. U and Th content rates increase with accessory minerals such as orthite or allanite, monazite, zircon, apatite, and sphene. These accessory minerals are mainly found in granitic rocks [27–29].

2. Geologic Setting

The study area lies in the Northwestern segment of the Abu Dabbab area, Central Eastern Desert of Egypt, nearby the northern bank of Marsa Alam City. It forms a part of the Upper Proterozoic Basement Complex between the intersection of the latitude 25°21′09.3″ N and longitude 34°3′29.1″ E (Figure 1). Three main wadis (valleys) are draining the Abu-Dabbab area; Wadi Mubarak, Wadi Abu Dabbab, and Wadi Dubr. Historically, the Abu Dabbab area means the area of sound tremor, due to frequent falling blocks as named by the desert inhabitants. The falling block phenomenon is assigned to the effect of active tectonics. The Abu Dabbab, Nuweibi, Muelha, Um Naggat, and Abu Rusheid localities are considered the famous occurrences of this mineralization, which reach the economic level [30].

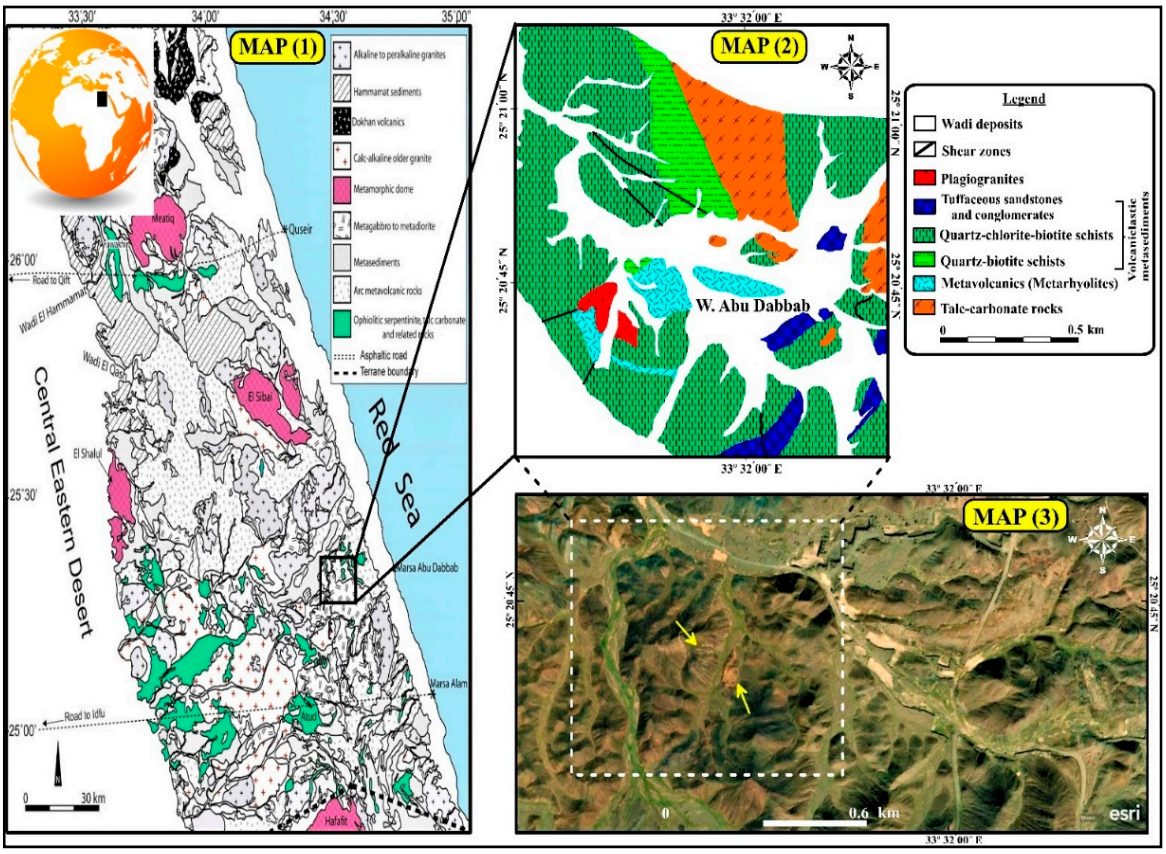

Figure 1. Map (**1**) Geological map for the Central Eastern Desert of Egypt, showing the Neoproterozoic basement rocks (modified from CONOCO map 1:500,000 and compiled from two quadrangle maps: Quseir quadrangle NG 36 NE and Gabal Hamata quadrangle NG 36 SE). Map (**2**) Detailed geologic map of the western part of Abu Dabbab area (modified after [31]). Map (**3**) The Google Earth imagery of Abu-Dabbab region; the yellow arrows are pointed to the plagio-granite location (central left).

Abu Dabbab has been subjected to many studies [31–37] because it is not far from Marsa Alam on the Red Sea coast and the presence of apo granites (metasomatized granites) as well as its enrichment with economic elements such as Ta, Nb, Sn, Cu, W, and Be (greisen deposits). The Abu Dabbab mapped area covers about 2 km^2. Its three main rock successions are the ophiolitic sequence (the oldest), island arc assemblage, and rare metal-bearing albite granite (the youngest). The ophiolitic assemblage (1.6 km^2) comprises exotic blocks of serpentinites and talc carbonate rocks. Island arc rocks include metasediments and metavolcanics, respectively. The metasediments comprise schists, meta sandy-siltstones,

and metagraywackes. The metavolcanics are composed mainly of meta basalts and meta rhyolite, occasionally associated with their tuffs.

The granite rocks along Wadi Abu Dabbab comprise tonalite, alkali feldspar granites, and apo granites, emplaced in Upper Proterozoic metasediments, metavolcanics, serpentinites, and metagabbros. The tonalite is of a relatively limited occurrence being restricted only to the north-western and south-western corners of the area. The contacts of tonalites at the north-western corner is concordant with the bedding of the metasediments [34]. Age determinations on the granites from Abu Dabbab and Nuweibi remained imprecise [38], but the emplacement of the intrusions can be bracketed between 600 Ma and 450 Ma [39], and is thus related to post-orogenic magmatism in the ANS. Several previous studies have focused on the rare metals in apo granite of Wadi Abu Dabbab, while the present study focuses on the plagio-granite near the western part of Abu Dabbab area according to [40] Figure 1. Ref. [40] suggested that the tectonic evolution of the area was associated with volcanic activity, whereas [41] attributed Abu Dabbab seismicity to the subsurface volcanic environment of a cooling pluton.

The plagio-granite masses are leucocratic rocks exposed to a large uniform outcrop that cuts volcaniclastic metasediments (Schists; Figure 2), and it is typically medium- to coarse-grained, greyish white color (Figure 2A). The pluton is highly fractured and jointed mainly in the two directions of NE-SW and NW-SE. The contacts of the plagio-granites with volcaniclastic metasediments are mostly sharp and well defined, indicating passive epizonal emplacement (Figure 2B). They show discordance with the regional foliation of the volcaniclastic metasediments. Their emplacement was most probably influenced by major tectonic lineaments.

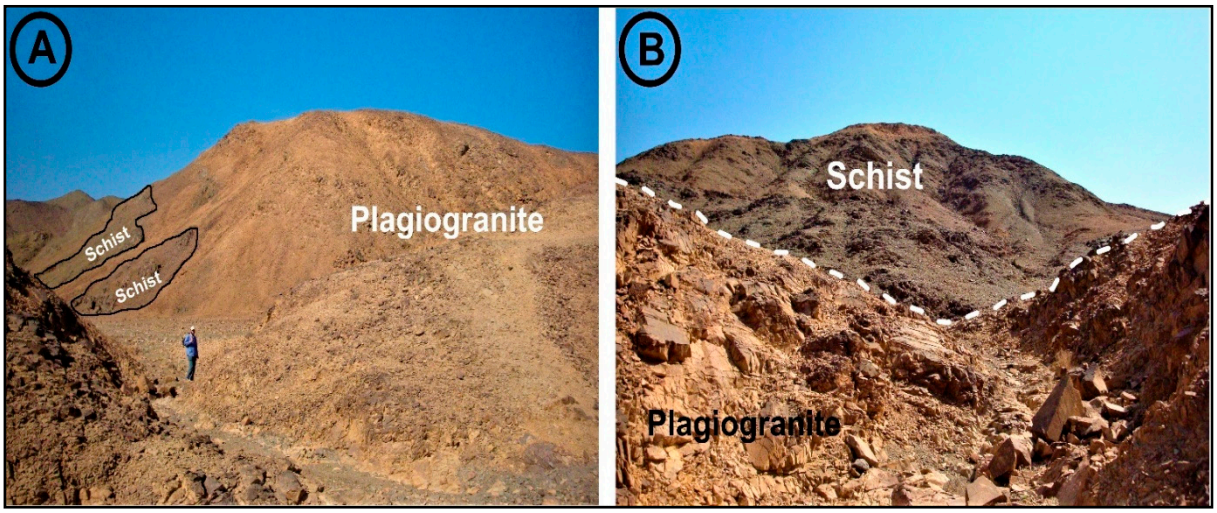

Figure 2. Field photographs of plagio-granite blocks encountered in Wadi Abu Dabbab. (**A**) Highly weathered plagio-granites. (**B**) Jointed plagio-granites intruded within volcaniclastic metasediments at Wadi Abu Dabbab.

3. Materials and Methods

Twenty-one samples were collected from Abu Dabbab plagio-granites for mineralogical and chemical analyses. Petrographic studies of thin sections were performed at the Laboratories of Al-Azhar University to identify the mineralogical composition and textures. Ten Abu Dabbab plagio-granite samples were selected for the geochemical study. Major oxides and some trace elements were determined by X-ray fluorescence at the Central Metallurgical Researching and Development Institute (CMRDI). Analytical precision determined on replicate analyses is generally better than ±5% for the major oxides and between ±5% and ±10% for minor and trace elements. The rare-earth elements (REEs) and several other trace elements were analyzed by inductively coupled plasma mass spectrometry at

the National Research Center (NRC), using a Na_2O_2 sintering technique. The precision is between ±2% and ±4%.

4. Results and Discussion

4.1. Petrography

Plagio-granites consist mainly of plagioclase and quartz; biotite and muscovite occurs as accessory minerals. Meanwhile, epidote, sericite, and carbonate minerals are secondary minerals. The textures of plagio-granites range from euhedral granular to granophyric intergrowths of plagioclase and quartz. Normative analyses of the studied plagio-granite samples fall in the tonalite field of the QAP diagram (along the quartz-plagioclase side; Figure 3).

Plagioclase (34%–49%) is mostly sodic (oligoclase) and forms a high value and large tabular subhedral crystals (Figure 4a). In plagioclase crystals, sericite, epidote, zoisite, and carbonate (calcite) are present as the alteration products of plagioclase which reflects a highly deformed effect (Figure 4b,c). Plagioclase grains enclose some crystals of carbonate, sericite, and epidote forming a poikilitic texture (Figure 4b,c). Quartz (38%–47%) is fine- to coarse-grained, subhedral to euhedral crystals, and polygonal crystals are often displayed with irregular edges (Figure 4d,e). It shows myrmekitic as well as micrographic textures. Patches of plagioclase are found intergrown within quartz forming wart-like shapes or the so-called myrmekitic texture (Figure 4f). The micrographic texture is common between K-feldspar and quartz (Figure 4g). In an extreme case, when the growth of myrmekite is vigorous in tonalite or plagiogranite with a minor amount of K-feldspar, all the K-feldspar crystals may be thoroughly eliminated or replaced by myrmekite, as if myrmekite can develop in a rock which was originally free of K-feldspar.

Biotite occurs as subhedral prismatic high relief and brown, strongly pleochroic from pale green to brown. It is slightly epidotized to completely alter epidote, muscovite, and chlorite (Figure 4h,i). Breakdown of brown biotite to green chlorite, opaque, and epidote suggests recrystallization. Muscovite is present in large amounts, although it is the most common mica after biotite. It occurs in clear flakes either as aggregates or as separate crystals associated with biotite (Figure 4h–j). Epidotes form pale yellow and purple granular aggregates (allotriomorphic crystals). Epidotization is a product of hydrothermal alteration and fills micropores of saussuritized plagioclase (Figure 4c) with biotite crystals (Figure 4h). Sericite chiefly occupies the central core of the plagioclase and the muscovite periphery (Figure 4b,c,j).

Carbonate minerals are present as an alteration product derived from calcium-bearing minerals (Ca-plagioclase and epidote). They are represented by calcite, which appears as two sets of cleavage with good twinkling (Figure 4k,l). Carbonatization occurs when susceptible rocks in the crust and mantle interact with CO_2-rich fluids resulting in the alteration and precipitation of carbonate and other minerals [42]. The Ca that forms calcite can be external in origin or remobilized from adjacent rocks. The source of carbonation fluids may be the result of (1) exsolution of carbonate fluids from cooling granite intrusions [43]; (2) submarine metamorphism at great depth, where H_2O and CO_2 were forced into slowly cooling lava as a result of great hydrostatic pressure [44]; (3) release of CO_2 from calcareous sediments during metamorphism [45,46]; and (4) degassing of a mantle source similar to that of carbonatites (Shimron et al., 1973).

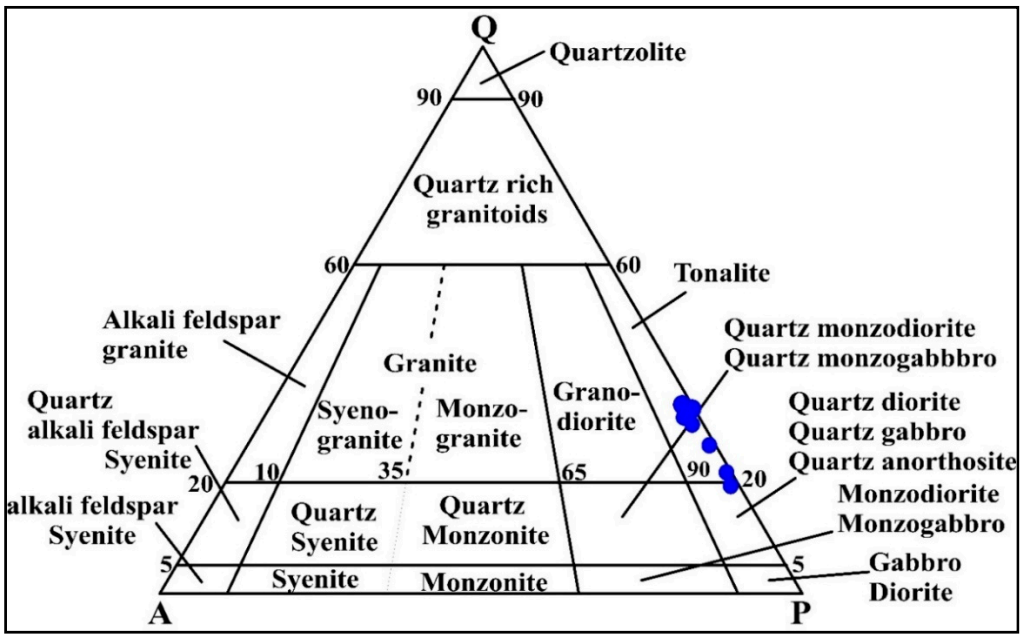

Figure 3. Classification of Abu Dabbab plagiogranites by using CIPW norms [47].

4.2. Whole-Rock Geochemistry

The chemical analyses of major oxides, trace, and rare earth elements of the Abu-Dabbab plagio-granites and their calculated normative mineral compositions are listed in Table 1. The present chemical analyses reveal SiO_2 (70.66–74.10 wt.%), TiO_2 (0.19–0.28 wt.%), Al_2O_3 (13.02–14.34 wt.%), K_2O (0.01–0.60 wt.%), Na_2O (6.57–9.98 wt.%), MgO (0.51–0.61 wt.%), CaO (1.31–1.81 wt.%) and LOI (0.60–1.02 wt.%). Abu-Dabbab plagio-granites are characterized by high SiO_2 and Na_2O contents. Well-preserved igneous textures and relatively low loss on ignition (LOI) values indicate that the plagio-granite samples have undergone only weak alteration, and therefore the geochemical data largely reflect the primary composition of the rocks. Low K_2O content (0.01–0.60 wt.%) is a significant chemical characteristic of Abu-Dabbab plagio-granites. The high Na_2O values of the plagio-granites are probably due to plagioclase accumulation (albitization). Many workers suggest that the high Na_2O and low K_2O contents in plagio-granites are due to exchange with seawater [48]; Ref. [9] or late magmatic vapor-phase transport and removal of K_2O [49].

The abnormal SiO_2, Na_2O, and CaO contents in plagio-granite samples could be referred to as the effect of alteration processes such as albitization, silicification, and carbonation [9]. Many authors such as [50]; Refs. [50,51] have distinguished between:

1. Low-Al plagio-granite (TTG-type; having < 15 wt.% Al_2O_3 at 70 wt.% SiO_2 < 200 ppm Sr, slightly enriched LREEs, and flat HREEs with a negative Eu-anomaly).
2. High-Al type plagio-granite (having Al_2O_3 contents > 15 wt% at 70 wt.% SiO_2, high Sr > 300 ppm, low Yb < 1.8 ppm, low Nb < 11 ppm, low to moderate K/Rb ratios < 750 ppm, enriched LREEs, depleted HREEs, and have no, or only a slight, Eu anomaly).

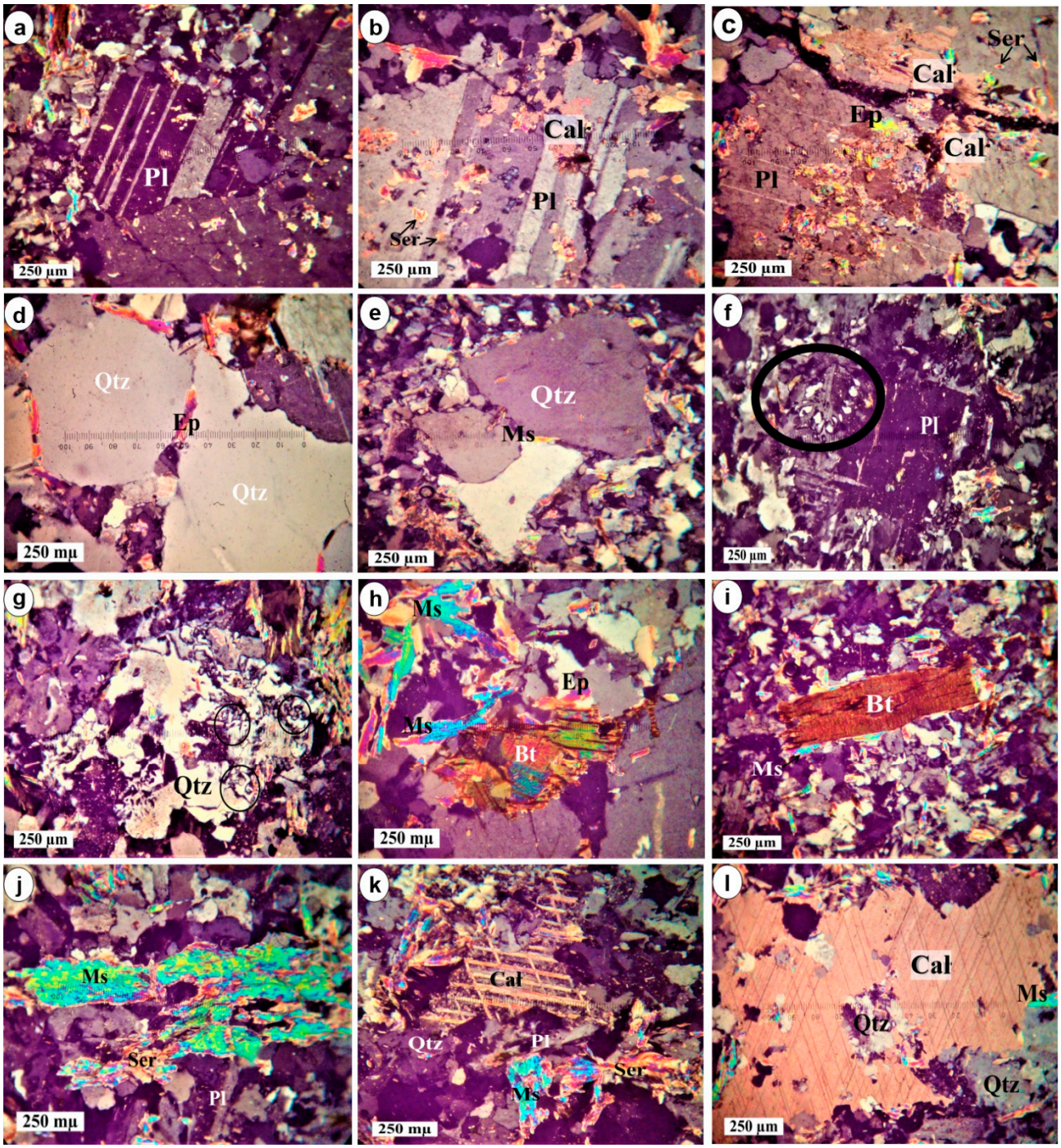

Figure 4. Photomicrographs showing the petrographic features of the Abu- Dabbab plagio-granites showing: (**a**) Subhedral plagioclase (Pl) altered to sericite (Ser). (**b**) Deformed plagioclase (Pl) crystals and poikilitic texture showing well developed crystals of sericite (Ser) and calcite (Cal). (**c**) Highly altered to saussurite (sericitization, carbonation, and epidotization). (**d**,**e**) Well undulose extinction of quartz (Qtz) exhibiting polygonal and porphyritic texture. (**f**) Myrmekitic texture resulting from intergrowing of quartz (Qtz) with sodic feldspar in plagio-granite (Pl). (**g**) Micrographic texture. (**h**,**i**) Large biotite crystal (Bt) altered to epidote (Ep) and muscovite (Ms). (**j**) Muscovite flakes (Ms) slightly altered to sericite (Ser). (**k**,**l**) Well-developed calcite (Cal) crystals exhibit good three sets of cleavage.

Table 1. Chemical analyses of Abu Dabbab plagio-granites.

	1a	1b	2a	2b	3a	3b	3c	4	9	10	AP1	AP2	AP3	AP4
Major Oxides (wt. %)														
SiO_2	73.36	73.12	74.10	71.18	70.66	71.12	73.07	73.69	72.14	70.81	72.21	74.10	64.60	72.39
TiO_2	0.22	0.21	0.20	0.28	0.23	0.19	0.21	0.23	0.23	0.28	0.22	0.27	0.12	0.18
Al_2O_2	14.01	13.02	13.21	14.04	13.91	13.75	14.01	14.25	14.34	13.49	13.79	13.73	13.21	15.08
Fe_2O_3	1.65	1.07	1.60	1.03	1.66	1.01	1.56	1.17	1.62	1.61	1.36	3.69	3.10	0.33
FeO	0.62	0.73	0.71	0.65	0.59	0.63	0.46	0.53	0.70	0.65	0.62	0.30	2.10	0.15
MnO	0.06	0.07	0.03	0.05	0.05	0.06	0.05	0.05	0.05	0.06	0.05	0.07	0.06	0.02
MgO	0.61	0.55	0.56	0.57	0.60	0.55	0.62	0.51	0.51	0.52	0.55	0.52	0.49	1.89
CaO	1.71	1.79	1.68	1.48	1.31	1.51	1.53	1.65	1.72	1.81	1.6	0.51	3.30	2.60
Na_2O	6.61	8.01	6.80	9.02	9.58	9.98	6.85	6.57	7.55	9.61	8.2	4.67	4.10	6.40
K_2O	0.02	0.10	0.32	0.13	0.60	0.17	0.22	0.08	0.11	0.01	0.17	1.59	2.20	0.28
P_2O_5	0.08	0.08	0.08	0.12	0.03	0.10	0.10	0.13	0.07	0.09	0.08	0.18	0.19	-
LOI	0.81	0.85	0.71	0.60	0.68	0.90	1.01	1.02	0.75	0.90	0.83	-	6.3	0.67
Total	99.76	99.60	100	99.15	99.90	99.97	99.69	99.88	99.79	99.84	99.77	99.63	99.77	99.99
Trace elements (ppm)														
V	21	17	22	14	20	24	18	19	18	17	19.45	-	-	-
Cr	4.11	4.95	4.51	6.05	5.21	4.62	6.01	4.21	5.52	4.38	4.92	-	-	15.17
Co	1.22	7.30	7.21	7.41	1.55	7.51	1.11	1.10	1	1.20	4.01	-	-	3.25
Rb	90	90	82	89	76	85	80	88	88	85	85.27	-	-	4.48
Ba	487	448	458	441	485	444	436	469	445	438	454.09	-	-	71.81
Sr	99	127	128	122	117	120	117	100	111	125	116.9	-	-	318.60
Nb	78	81	65	76	77	71	68	70	79	72	73.45	-	-	0.80
Ta	0.37	0.52	0.51	0.51	0.72	0.31	0.38	0.35	0.74	0.72	0.49	-	-	0.12
Zr	131	147	150	150	162	155	146	164	141	133	148.5	-	-	78.60
Hf	3.10	3	3	3	4	3.21	3	3.23	3.51	3	3.2	-	-	3.09
Y	30	38	34	31	20	30	22	24	30	23	28.36	-	-	5
Pb	58	65	52	59	49	55	57	60	62	55	57	-	-	
Cu	7	9	7	11	9	8	8	10	7	8	8.36	-	-	
Zn	42	42	36	44	41	44	50	43	42	38	42.36	-	-	14.20
U	4.7	5.07	4.9	6.01	6.2	5.8	5	6.2	4.7	5	5.39	-	-	0.31
Th	14.3	13.07	14.8	16.08	16.1	15.5	15.1	16.4	14.8	15.2	15.16	-	-	1.98
Rare earth elements (ppm)														
La	75	78	81	75	80	74	88	74	77	69	77.1	-	-	2.20
Ce	175	158	171	168	175	155	167	145	152	165	163.1	-	-	4.84
Pr	4	4	4	4	4	6	4	6	6	7	4.9	-	-	0.78
Nd	76	84	81	78	61	64	55	64	63	71	69.7	-	-	3.58
Sm	10	16	11	14	11	12	12	15	10	11	12.2	-	-	0.89
Eu	1	1	1	1	1	1	1	1	1	1	1	-	-	0.31
Gd	3	6	5	4	5	6	6	6	4	5	5	-	-	0.83
Tb	1	1	1	1	1	1	1	1	1	1	1	-	-	0.12
Dy	3	4	4	3	5	3	3	4	5	5	3.9	-	-	0.74
Ho	1	1.20	1	1.80	1	0.84	1	0.85	0.86	0.81	1.04	-	-	0.16
Er	1	1	1	1	1	1	1	1	1	1	1	-	-	-
Tm	0.30	0.71	0.34	0.35	0.41	0.38	0.37	0.44	0.71	0.79	0.48	-	-	0.09
Yb	2	2	2	3	2	1	2	2	1	2	1.9	-	-	0.52
Lu	1	1	1	1	1	1	1	1	1	1	1	-	-	0.09
CIPW norm														
Albite	55.5	65.87	57.12	70.86	69.16	57.54	55.21	55.5	63.3	68.73	-	-	-	-
Anorthite	7.90	-	4.54			6.78	7.29	6.2	4.87	-	-	-	-	-
Apatite	0.17	0.17	0.17	0.26	0.22	0.22	0.28	0.30	0.15	0.19	-	-	-	-
Corundum	0.20	-	-	-	-	-	-	-	-	-	-	-	-	-
Hematite	0.57	-	0.35	-	-	0.84	0.34	0.34	0.41	-	-	-	-	-
Ilmenite	0.41	0.40	0.38	0.53	0.36	0.40	0.43	0.44	0.43	0.53	-	-	-	-
Magnetite	1.55	0.94	1.79	-	-	1.03	1.20	1.20	1.74	-	-	-	-	-
Orthoclase	0.12	0.59	1.88	0.76	1	1.29	0.47	3.09	0.64	0.06	-	-	-	-
Quartz	30.27	23.38	29.60	17.03	16.80	28.28	31.02	29.62	24.0	18.79	-	-	-	-
Diopside	-	4.02	2.50	4.57	4.71	0.08	-	-	2.44	4.34	-	-	-	-
Wollastonite	-	1.38	-	0.37	0.43	-	-	-	-	1.25	-	-	-	-
Acmite	-	1.19	-	2.95	2.90	-	-	-	-	4.62	-	-	-	-
Hyperthene	1.51	-	0.23	-	-	1.49	1.26	1.27	0.13	-	-	-	-	-
Corundum	-	-	-	-	-	-	0.66	0.19	-	-	-	-	-	-

Ap1 = Average of Abu-Dabbab plagio-granites. Ap2 = Average of El Sukkari plagio-granites, Central Eastern Desert of Egypt [52]. Ap3 = Average of Hariari plagio-granites, Southeastern Desert of Egypt [53]. Ap4 = Average of Ashin plagio-granites, Central Iran [54].

Abu Dabbab plagio-granites do exhibit these chemical signatures, including low Al_2O_3 contents of 13.76 wt% at 72.21 wt.% silica, thus representing a low-alumina TTG suite. The characterization of the chemical components in the studied district will be considered compared to that of the El-Sukkari plagio-granites [52], Hariari plagio-granites [53], and Ashin plagio-granites [54]; (Table 1). The Sukkari plagio-granites are geochemically characterized by high SiO_2, K_2O, and Fe_2O_3 but depleted in Na_2O compared with Abu-Dabbab plagio-granite given in Table 1. Meanwhile, the present samples are chemically like the Ashin plagio-granites, which have a low content of Al_2O_3, MgO, and CaO, in addition to being rich in Fe_2O_3 and Na_2O values compared with Ashin plagio-granites. Hariari plagio-granites exhibit high values of Fe_2O_3, FeO, Al_2O_3, CaO, K_2O, and LOI compared with Abu-Dabbab plagio-granites. Furthermore, the concentration of Ba (436–487 ppm with an average 454.09 ppm), Sr (99–128 ppm with an average 116.90 ppm), Zr (131–164 ppm with an average 148.5 ppm), Rb (76–90 ppm with an average 85.27 ppm), Nb (65–81 ppm with an average 73.45 ppm), Ce (145–175 ppm with an average 163.1 ppm), and Nd (55–84 ppm with an average 69.7 ppm) are high in Abu-Dabbab plagio-granites.

The chemical analyses of the plagio-granites were used to calculate the CIPW norm (Table 1). The CIPW normative minerals were calculated after Hutchison and Lumpur (1975). The normative mineral composition of the studied Abu-Dabbab plagio-granites shows high values of quartz (16.80% to 31.02%), orthoclase (0.12% to 3.09%), anorthite (4.54% to 7.90%), albite (55.21% to 70.86%), hypersthene (0.13% to 1.49%), and diopside (0.08% to 4.57%). They also show low contents of apatite (0.15% to 0.30%), ilmenite (0.36% to 0.53%), and magnetite (1.03% to 1.79%). The presence of normative corundum in some samples (3c and 4) of the plagio-granite may be due to the alteration of plagioclase which transports alkalis and leaves alumina. Moreover, the normative mineral compositions reveal that oversaturated plagio-granites are present in the studied samples, which are classified as oversaturated (quartz-normative). This would suggest that all the analyzed plagio-granites are calc-alkaline in nature. However, the use of normative mineral compositions is highly influenced by the effects of secondary alteration.

A reasonable correlation with the presumed order of magmatic evolution is given through major element variation diagrams (Figure 5). According to Harker's variation diagrams of Abu Dabbab plagio-granite samples, SiO_2 values show a slightly positive correlation with CaO and La. On the other hand, clear negative correlation with Al_2O_3, TiO_2, K_2O, Na_2O, and Th (Figure 5). MgO and Zr exhibit no systematic variation. The CaO-Na_2O-K_2O ternary diagram of [55], (Figure 6A) shows that the plotted plagio-granite samples fall in the tonalite field. On the anorthite-orthoclase-albite normative diagram of [56] and (albite-anorthite-orthoclase) diagram of [57]; the present samples plot within the compositional fields of trondhjemites (Figure 6B,C). On the variation diagram of La/Yb versus Yb after [58], the plagio-granite samples are plotted on Archaean tonalite-trondhjemite-granodiorite suits and adakites field (Figure 6D). All plagio-granite samples have a variation in plagioclase composition ranging from oligoclase to albite (Figure 7).

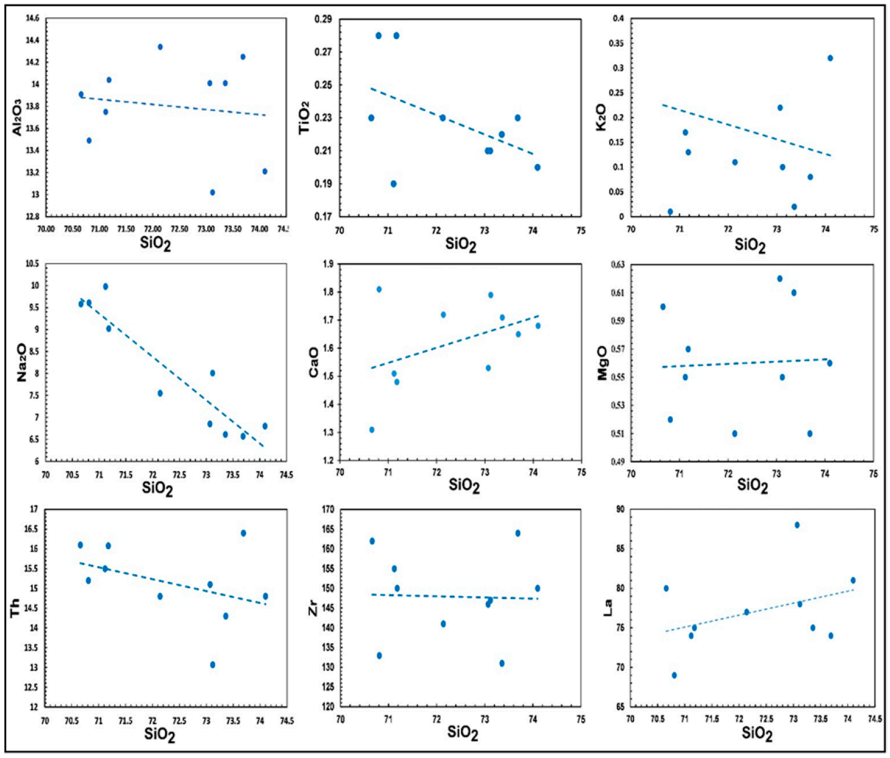

Figure 5. Harker variation diagrams of Abu-Dabbab plagio-granites.

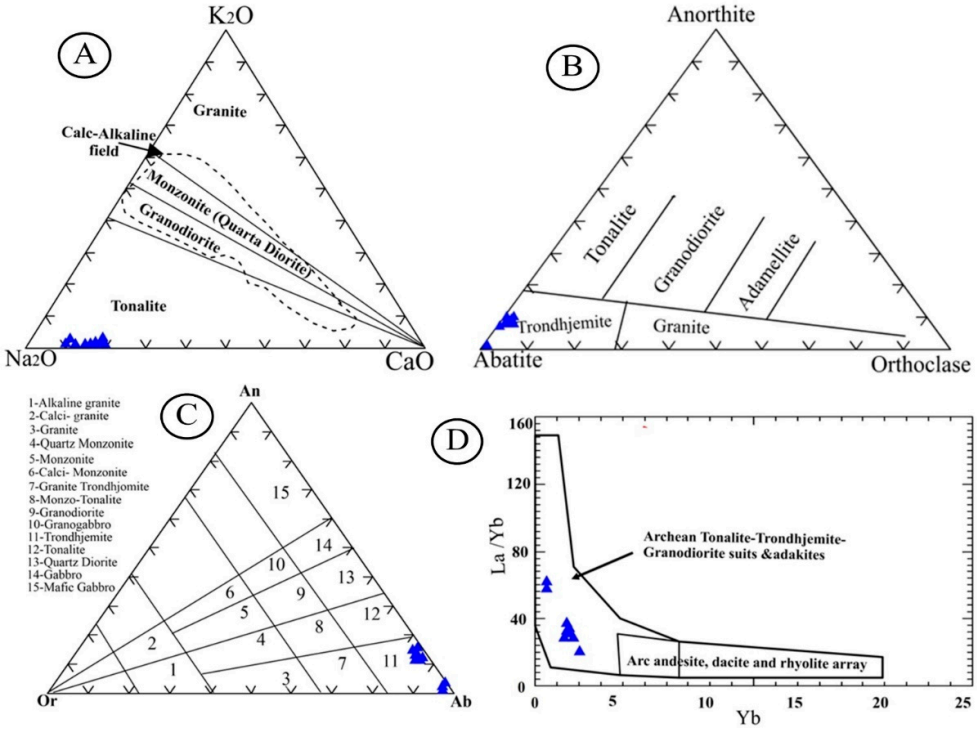

Figure 6. Geochemical classification of the Abu Dabbab plagio-granites. (**A**) The CaO-Na_2O-K_2O ternary diagram of [55] for the Abu Dabbab plagio-granites. (**B**) CIPW normative classification of the analyzed Abu-Dabbab plagio-granites, after [57] and modified by [59]. (**C**) Or-An-Ab ternary diagram of [56] for the Abu Dabbab plagio-granites. (**D**) La/Yb-Yb diagram shows the Abu Dabbab plagio-granites, after [58].

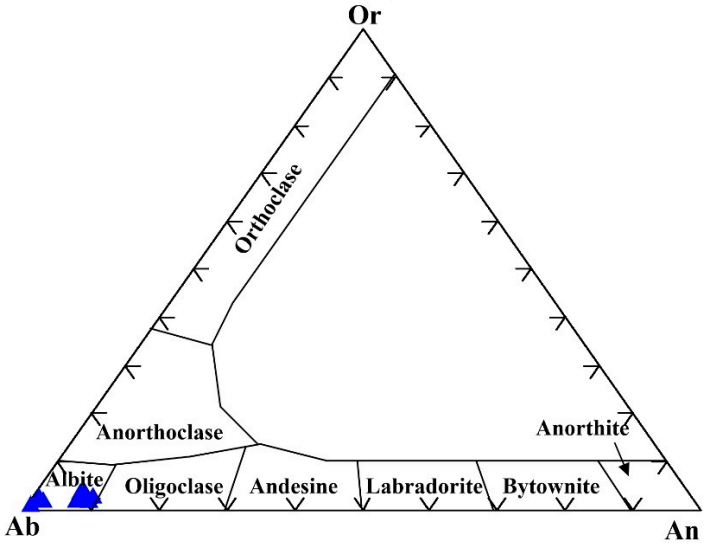

Figure 7. Feldspar (anorthite [An]-albite [Ab]-orthoclase [Or]) compositional diagram to nomenclature the plagioclase series [60].

4.3. Petrogenesis

According to [9] in their review of the plagio-granites in general, the latter differs from most other granitic rocks in having very low potassium content and heavy REE distributions that resemble those of mid-ocean ridge basalts (MORBs). However, it must be admitted that such rocks are not easy to study geochemically, owing to the effects of extensive hydrothermal leaching, as noted in the Abu Dabbab area example, which possibly accounts for the low potassium.

Ref. [61] suggested that a semi-log plot of SiO_2 versus K_2O (Figure 8) illustrates the nature of the extremely low potassium content in these rocks compared with continental basalts and they are different. In this diagram, most plagio-granite samples plot in the oceanic plagio-granite field (Figure 8A). According to La versus La/Sm diagram after [62], the plotted samples trends indicate that partial melting may have played an important role in the origin of the Abu-Dabbab plagio-granites (Figure 8B). The binary relationship between TiO_2 and SiO_2 of Abu-Dabbab plagio-granites supports a partial melting origin. This is also agreeing with the behavior of data on La against La/Sm diagrams [62]; (Figure 8C).

Abu-Dabbab plagio-granite samples plot within the field of volcanic arc granite, as reinforced by the (Rb/10)-Hf-(3Ta) discrimination diagram (Figure 9); [63] These results support the theory put out by [14] that some plagio-granite 350 samples found in the Onib ophiolite are silica-rich and have low levels of Nb and Y, similar to samples from the 351 volcanic arc samples, which may explain the origin of the Onib ophiolite as a back-arc. According to [13], the present samples fall nearby the back arc basin (Figure 10). Figure 11 shows the spidergram of an oceanic plagio-granite according to (CI chondrite [64] and Primitive mantle [65]. The pattern indicates:

- The slightly enriched patterns of the LREEs in the studied plagio-granites as well as the negative anomalies of Eu, Sr, Y, and Ta; low concentrations of HREEs indicate that they were likely derived from the partial melting in a subduction zone;
- Greater enrichment in Pb, Nb, Ba, Rb, and light rare earth elements (LREEs) than for HREEs.

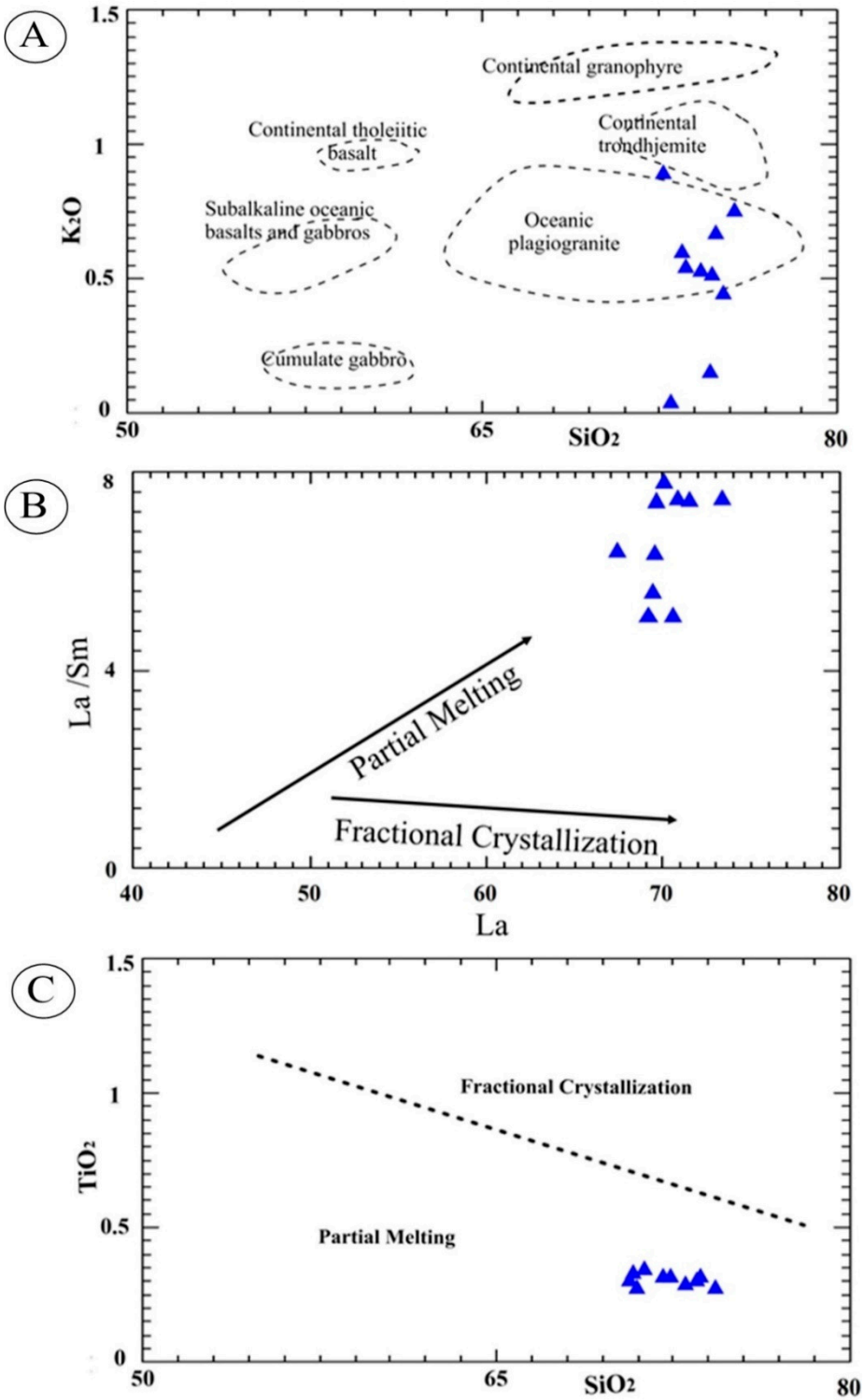

Figure 8. (**A**) Semi log plot of SiO_2 versus K_2O [61] and location of the studied Abu Dabbab plagio-granite samples. (**B**) Plots of La versus La/Sm for the Abu Dabbab plagio-granites [62]. (**C**) SiO_2 versus TiO_2 [66].

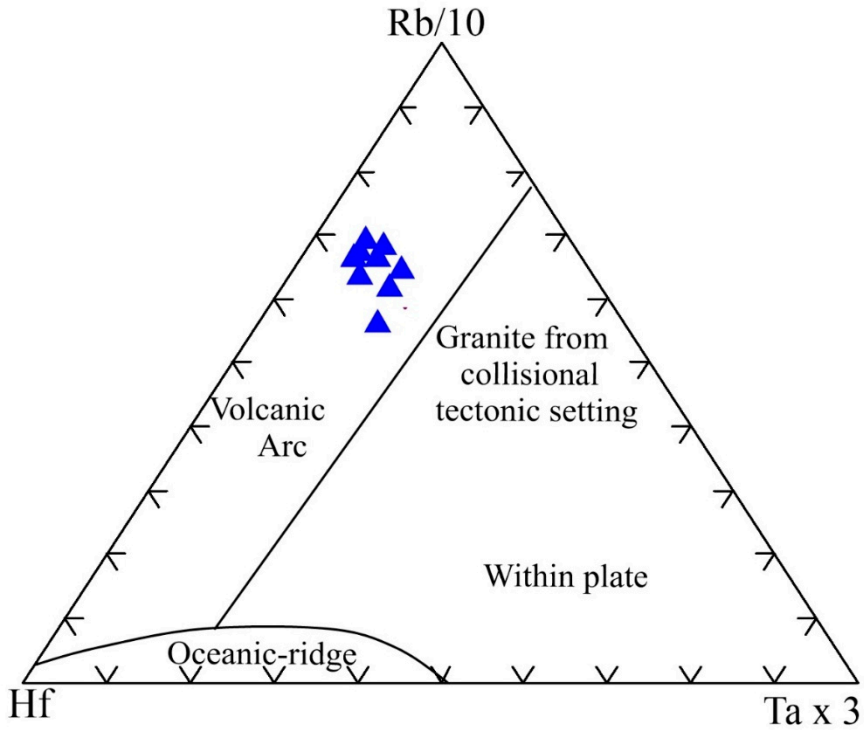

Figure 9. Rb/10-Hf- Ta x 3 discrimination diagram [67], identifying tectonic setting.

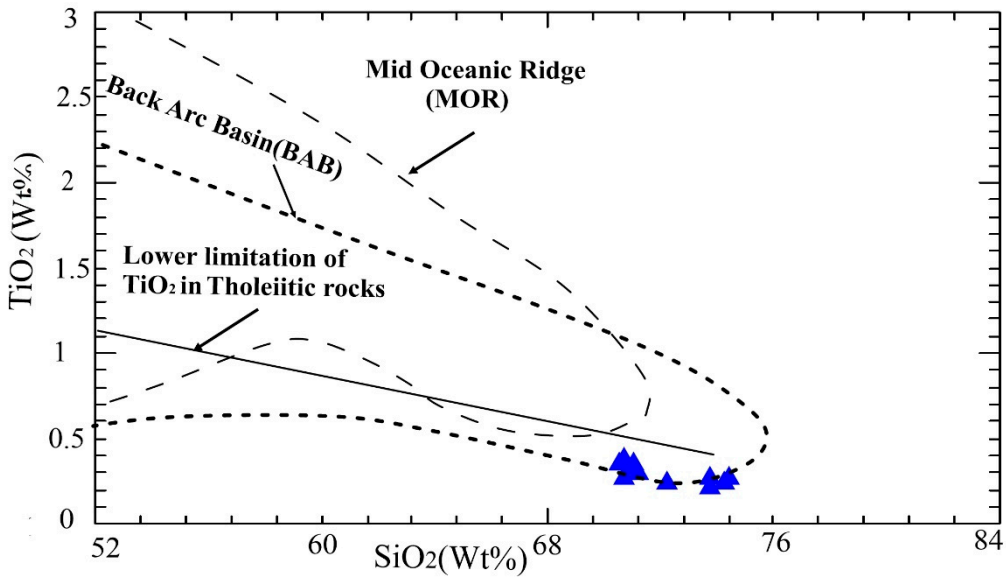

Figure 10. TiO_2 versus SiO_2 the samples plot near the border of magma differentiation and melts released from partial melting [66].

4.4. Natural Radioactive Elements:

U content in plagio-granites ranges from 0.3 to 6.2 ppm, with an average up to 4.9 ppm, while its Th content ranges from 1.98 to 16.4 ppm, with an average up to 14.0 ppm. On the other hand, Sm and Rb contents are ranging from (1.1 to 1.6 with average 1.2 ppm and 0.45 to 0.52 with average 0.5 ppm, respectively). The contents of U and Th of ore metals are ranging from 1.6 to 2.1 ppm with an average of 1.8 ppm, and 0.8 to 1.0 with an average of 0.9 ppm, respectively, as shown in Tables 1 and 2. Plagio-granites and ore metal samples are hence considered non-uraniferous according to [68] because their U content is greatly less than the Clark value of U (4 ppm) characterizing normal non-uraniferous granites.

Mostly, high U content is attributed to the presence of accessory and secondary minerals, such as monazite, zircon, and kasolite [29].

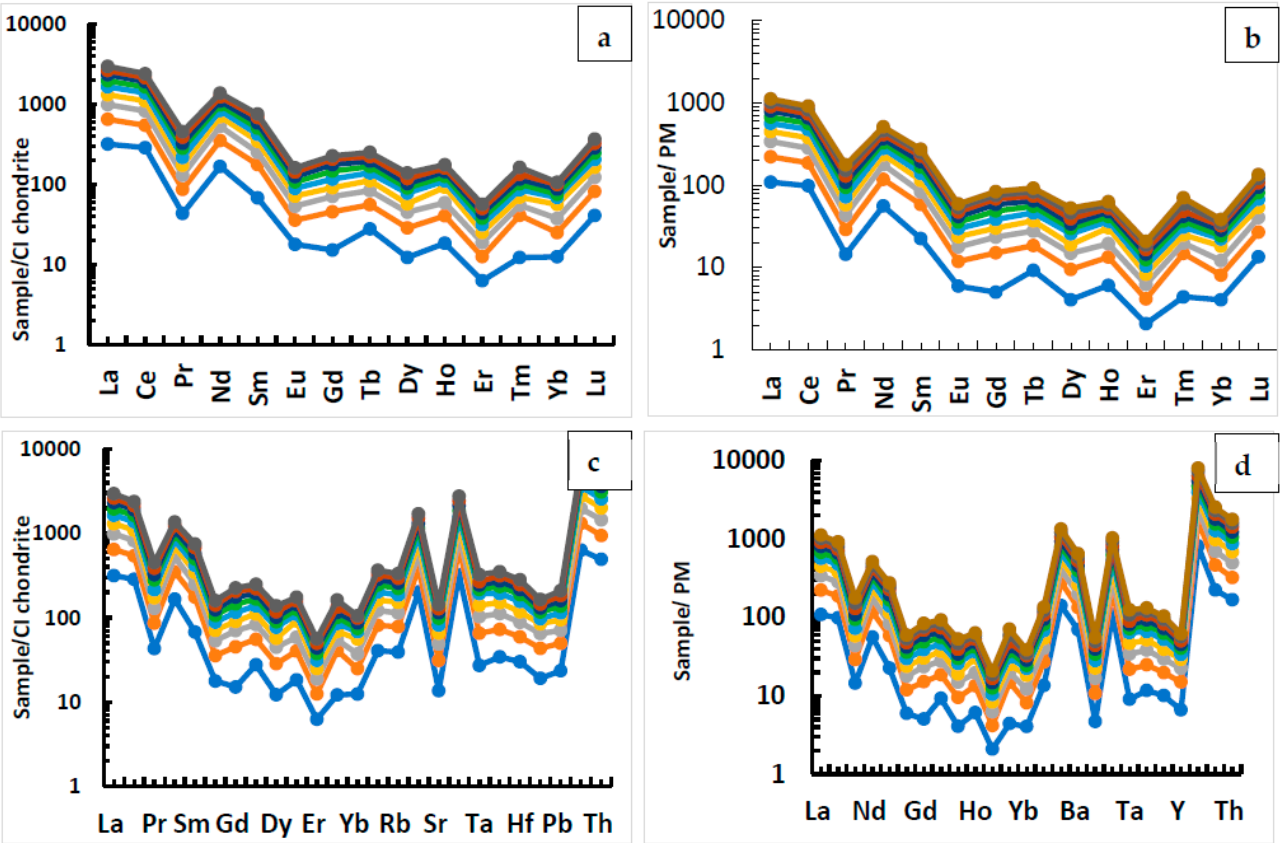

Figure 11. (**a**) REE-Chondrite normalized [64] (**b**) REE-Primitive mantle [65] spider diagrams of plagio-granite. (**c**) Chondrite normaslized of trace-REE pattern compositions of Abu Dabbab plagio-granites (after [64]). (**d**) Primitive mantle normalized of trace-REE pattern compositions of Abu Dabbab plagio-granites (after [65]).

4.5. Clarke Concentration

The Clarke concentration (CC) was calculated by dividing the concentration of the different elements in the studied plagio-granite samples by the reference values for these elements. The reference values of the elements are given by [69]. The content of the element in the rocks is normal when CC value fluctuated between 0.5 and 1.78 [70]. The elements having CC value less than 0.5 or more than 1.78 is to be considered negatively or positively anomalous, respectively. The results of the chemical analysis of the studied plagio-granite samples are given in Table 2.

The Clarke concentration values of Abu Dabbab plagio-granite show that V, Rb, Ta, Gd, Er, and Yb are negatively anomalous (less than 0.5). Meanwhile, the CC values of Ba, Zr, Hf, Y, Cu, Th, Pr, Eu, Tb, Tm, Dy, Ce, and Ho are normal (CC values > 0.5 < 1). Plagio-granite samples show a high concentration value for Co, Nb, Pb, U, and Nd (more than 1.88). The plagio-granite is exposed as a large uniform outcrop located near the western portion of the Abu Dabbab area. The plagio-granites are composed essentially of plagioclase and quartz as main constituents. Meanwhile, biotite and muscovite are present as accessory minerals as well as epidote, sericite, and calcite are secondary minerals. The textures of plagio-granites range from euhedral granular to granophyric intergrowths of plagioclase and quartz, and myrmekitic and micrographic textures. A high value of plagioclase is evident in the petrography of the studied plagio-granites. This reflects the slight effect of

the albitization alteration processes. The alteration types are albitization, sericitization, epidotization, kaolinitization, and carbonatization.

Table 2. Concentration Clarke (cc) values of some ore metals collected from Abu Dabbab plagio-granites.

Trace elements											
S.No.	1a	1b	2a	2b	3a	3b	3c	4	9	10	Av.
V	0.48	0.39	0.50	0.32	0.45	0.55	0.41	0.43	0.41	0.39	0.43
Cr	1.00	1.18	1.05	1.38	1.16	1.00	1.28	0.88	1.13	1.07	1.11
Co	1.22	7.30	7.21	7.41	1.55	7.51	1.11	1.10	1.00	1.20	3.66
Rb	0.53	0.53	0.48	0.52	0.45	0.50	0.47	0.52	0.52	0.50	0.50
Ba	0.58	0.53	0.55	0.53	0.58	0.53	0.52	0.56	0.53	0.52	0.54
Sr	0.99	1.27	1.28	1.22	1.17	1.20	1.17	1.00	1.11	1.25	1.17
Nb	3.71	3.86	3.10	3.62	3.67	3.38	3.24	3.33	3.76	3.43	3.51
Ta	0.09	0.13	0.13	0.13	0.18	0.08	0.10	0.09	0.19	0.18	0.13
Zr	0.75	0.84	0.86	0.86	0.93	0.89	0.83	0.94	0.81	0.76	0.85
Hf	0.74	0.71	0.71	0.71	0.95	0.76	0.71	0.77	0.84	0.71	0.76
Y	0.75	0.95	0.85	0.78	0.50	0.75	0.55	0.60	0.75	0.58	0.71
Pb	3.05	3.42	2.74	3.11	2.58	2.89	3.00	3.16	3.26	2.89	3.01
Cu	0.7	0.9	0.7	1.1	0.9	0.8	0.8	1.0	0.7	0.8	0.84
Zn	1.08	1.08	0.92	1.13	1.05	1.13	1.28	1.10	1.08	0.97	1.08
U	1.6	1.7	1.6	2.0	2.1	1.9	1.7	2.1	1.6	1.7	1.80
Th	0.8	0.8	0.9	0.9	0.9	0.9	0.9	1.0	0.9	0.9	0.89
Rare earth elements											
La	1.36	1.42	1.47	1.36	1.45	1.35	1.60	1.35	1.40	1.25	1.40
Ce	1.90	1.72	1.86	1.83	1.90	1.68	1.82	1.58	1.65	1.79	1.77
Pr	0.45	0.45	0.45	0.45	0.45	0.68	0.45	0.68	0.68	0.80	0.56
Nd	2.05	2.27	2.19	2.11	1.65	1.73	1.49	1.73	1.70	1.92	1.88
Sm	1	1.6	1.1	1.4	1.1	1.2	1.2	1.5	1	1.1	1.22
Eu	0.63	0.63	0.63	0.63	0.63	0.63	0.63	0.63	0.63	0.63	0.63
Gd	0.3	0.6	0.5	0.4	0.5	0.6	0.6	0.6	0.4	0.5	0.5
Tb	0.63	0.63	0.63	0.63	0.63	0.63	0.63	0.63	0.63	0.63	0.63
Dy	0.42	0.56	0.56	0.42	0.69	0.42	0.42	0.56	0.69	0.69	0.54
Ho	0.50	0.60	0.50	0.90	0.50	0.42	0.50	0.43	0.43	0.41	0.52
Er	0.25	0.25	0.25	0.25	0.25	0.25	0.25	0.25	0.25	0.25	0.25
Tm	1.00	2.37	1.13	1.17	1.37	1.27	1.23	1.47	2.37	2.63	1.60
Yb	0.5	0.5	0.5	0.75	0.5	0.25	0.5	0.5	0.25	0.5	0.48
Lu	0.83	0.83	0.83	0.83	0.83	0.83	0.83	0.83	0.83	0.83	0.83

There are different ways for plagio-granites formation within the geological history of the Oman ophiolite. (1) Early plagio-granites associated were produced by the partial melting of hornblende gabbros; these are the "high level intrusive" of [71]. (2) Late intrusive complexes of plagio-granites ± gabbros formed from a mafic magma by the re-melting of previously depleted mantle harzburgite (after [71]). (3) Plagio-granites intrusive into mantle peridotites [72]. They are strongly enriched in light REEs and fluid-mobile elements and contain components from both crustal and mantle sources [7]. The enrichment in these elements (Co, Nb, Pb, U, and Nd) may be likely a configuration of plagio-granite from partial melting of highly depleted mantle harzburgite and pre-existing oceanic crustal rocks (basalts and/or gabbros). The geochemical anomalies for the different elements in the Abu Dabbab plagio-granite are mainly present within the internal structure of the mineral constituents of these plagiogranites. It reflects the epigenetic of the mineralization during the magmatic crystallization of the plagio-granites.

5. Conclusions

Geochemically, the plagio-granites rocks are mainly tonalite or trondhjemite in composition. Abu Dabbab plagio-granite exhibit these chemical signatures, revealing low

Al_2O_3 contents of 13.76 wt.% at 72.21 wt.% silica, thus representing a low-alumina TTG suite. Plagio-granite samples have a peraluminous behavior and differentiate between calc-alkaline and tholeiitic affinity. According to the REEs analysis, the samples seem to be oceanic plagio-granite and of a partial melting origin. Geochemical data of the plagio-granite characterized by a wide range of SiO_2 and Na_2O has moderate enrichment in Pb, Rb, Nb, HREEs, and depletion in Ta, Sr, Y, and HREEs. The major oxides, trace, and rare earth elements values show that Abu Dabbab plagio-granites belong to the low-K series of ophiolitic complexes and reveal geochemical characteristics with the ocean ridge granites. Abu Dabbab plagio-granite samples exhibit a high Clarke concentration value for Co, Nb, Pb, U, and Nd (more than 1.88). The high CC values in these elements may support the study of plagio-granite derived from partial melting of highly depleted mantle harzburgite, pre-existing oceanic crustal rocks (basalts and/or gabbros).

Author Contributions: Conceptualization, H.M.E.-D. and A.M.A.-R.; data curation, H.A.A., H.M.H.Z. and A.E.; formal analysis, H.M.E.-D., W.F., A.E.K. and H.A.A.; funding acquisition, A.E.; investigation, A.M.A.-R., H.A.A., H.M.H.Z., W.F., A.E.K. and A.E.; methodology, H.M.E.-D. and A.M.A.-R.; project administration, H.A.A., H.M.H.Z. and A.E.; resources, H.M.E.-D., A.M.A.-R. and W.F.; software, W.F., A.E.K. and W.F.; supervision, H.M.E.-D., H.A.A., A.M.A.-R. and A.E.; validation, A.M.A.-R., H.A.A., H.M.H.Z., W.F. and A.E.; visualization, H.A.A. and H.M.H.Z.; writing—original draft, H.M.E.-D., H.A.A. and A.M.A.-R.; writing—review and editing, H.A.A., H.M.H.Z., H.M.E.-D., A.M.A.-R. and A.E. All authors have read and agreed to the published version of the manuscript.

Funding: The APC is funded by "Dunarea de Jos" University of Galati, Romania.

Data Availability Statement: Not applicable.

Acknowledgments: The researcher (H.A.A.) is funded by a scholarship under the Joint (Executive Program between Egypt and Russia) The author is deeply indebted to Mahmoud M. Hassaan, Geology Department, Faculty of Science, Al-Azhar University for proposing the point of the study.

Conflicts of Interest: The authors declare no conflict of interest.

References

1. Coleman, R.G.; Peterman, Z.E. Oceanic plagiogranite. *J. Geophys. Res.* **1975**, *80*, 1099–1108.
2. Gillis, K.M.; Coogan, L.A. Anatectic migmatites from the roof of an ocean ridge magma chamber. *J. Petrol.* **2002**, *43*, 2075–2095. [CrossRef]
3. Rollinson, H. The geochemistry of mantle chromitites from the northern part of the Oman ophiolite: Inferred parental melt compositions. *Contrib. Miner. Pet.* **2008**, *156*, 273–288.
4. Tsuchiya, N.; Shibata, T.; Yoshikawa, M.; Adachi, Y.; Miyashita, S.; Adachi, T.; Nakano, N.; Osanai, Y. Petrology of Lasail plutonic complex, northern Oman ophiolite, Oman: An example of arc-like magmatism associated with ophiolite detachment. *Lithos* **2013**, *156–159*, 120–138.
5. Awad, H.A.M.; Nastavkin, A.V. Some Mechanical and Physical Studies of Granitic Rocks in Um Taghir, Eastern Desert, Egypt. *J. Phys. Conf. Ser.* **2021**, *1945*, 012012.
6. Awad, H.A.; Nastavkin, A.V. Geochemical and Geotectonic Setting for Island Arc Related rocks on Um Taghir Area, Central Eastern Desert, Egypt. *IOP Conf. Ser. Earth Environ. Sci.* **2021**, *720*, 012049.
7. Rollinson, H. New models for the genesis of plagiogranites in the Oman ophiolite. *Lithos* **2009**, *112*, 603–614.
8. Stakes, D.S.; Taylor, H.P., Jr. Oxygen isotope and chemical studies on the origin of large plagiogranite bodies in northern Oman, and their relationship to the overlying massive sulphide deposits. *Geol. Soc. Lond. Spec. Publ.* **2003**, *218*, 315–351.
9. Coleman, R.G.; Donato, M.M. Oceanic plagiogranite revisited. *Dev. Petrol.* **1979**, *6*, 149–168.
10. Dixon, J.E.; Lippard, S.J.; Shelton, A.W.; Gass, I.G. *The Ophiolite of Northern Oman*; Basil Blackwell: Oxford, UK, 1986.
11. Malpas, J. Two contrasting trondhjemite associations from transported ophiolites in Western Newfoundland: Initial report. *Dev. Petrol.* **1979**, *6*, 465–487.
12. Huang, S.; Wang, W.; Kerr, A.C.; Zhao, J.; Xiong, Q.; Wang, J. The Fuchuan Ophiolite in South China: Evidence for Modern-Style Plate Tectonics During Rodinia Breakup, Geochemistry, Geophys. *Geosystems* **2021**, *22*, e2021GC010137.
13. Koepke, J.; Feig, S.T.; Snow, J.; Freise, M. Petrogenesis of oceanic plagiogranites by partial melting of gabbros: An experimental study. *Contrib. Miner. Pet.* **2004**, *146*, 414–432.
14. Kröner, A.; Todt, W.; Hussein, I.M.; Mansour, M.; Rashwan, A. Dating of late Proterozoic ophiolites in Egypt and the Sudan using the single grain zircon evaporation technique. *Precambrian Res.* **1992**, *59*, 15–32.
15. Zhang, Q.; Wang, C.Y.; Liu, D.; Jian, P.; Qian, Q.; Zhou, G.; Robinson, P.T. A brief review of ophiolites in China. *J. Asian Earth Sci.* **2008**, *32*, 308–324.

16. Dilek, Y.; Furnes, H. Ophiolites and their origins. *Elements* **2014**, *10*, 93–100.
17. Li, W.-X.; Li, X.-H. Adakitic granites within the NE Jiangxi ophiolites, South China: Geochemical and Nd isotopic evidence. *Precambrian Res.* **2003**, *122*, 29–44. [CrossRef]
18. Freund, S.; Haase, K.; Keith, M.; Beier, C.; Garbe-Schönberg, D. Constraints on the formation of geochemically variable plagiogranite intrusions in the Troodos Ophiolite, Cyprus. *Contrib. Miner. Pet.* **2014**, *167*, 978.
19. Liu, L.; Kang, L.; Cao, Y.; Yang, W. Early Paleozoic granitic magmatism related to the processes from subduction to collision in South Altyn, NW China. *Sci. China Earth Sci.* **2015**, *58*, 1513–1522.
20. Yang, W.; Niu, H.; Hollings, P.; Zurevinski, S.E.; Li, N. The role of recycled oceanic crust in the generation of alkaline A-type granites. *J. Geophys. Res. Solid Earth* **2017**, *122*, 9775–9783.
21. Rahman, E.M.A. *Geochemical and Geotectonic Controls of the Metallogenic Evolution of Selected Ophiolite Complexes from the Sudan*; Selbstverlag Fachbereich Geowissenschaften: Berlin, Germany, 1993.
22. Patiño Douce, A.E.; McCarthy, T.C. Melting of crustal rocks during continental collision and subduction. In *When Continents Collide: Geodynamics and Geochemistry of Ultrahigh-Pressure Rocks*; Springer: Dordrecht, The Netherlands, 1998; Volume 10, pp. 27–55.
23. El Shazly, E.M. The geology of the Egyptian region. In *The Ocean Basins Margins*; Nairn, A.E.M., Kanes, W.H., Stehli, F.G., Eds.; Springer: Boston, MA, USA, 1977; pp. 379–444.
24. Gamal El Dien, H.; Li, Z.-X.; Abu Anbar, M.; Doucet, L.S.; Murphy, J.B.; Evans, N.; Xia, X.-P.; Li, J. The largest plagiogranite on Earth formed by re-melting of juvenile proto-continental crust. *Commun. Earth Environ.* **2021**, *2*, 138.
25. Hassaan, M.M.; El-Desoky, H.M. Granites in the tectonic environs of the Nubian Shield, Egypt: Geochemical characterizations and new contributions. *Curr Res.* **2016**, *10*, 59–103.
26. Wilson, M. *Igneous Petrogenesis*; Springer: Dordrecht, The Netherlands, 1989.
27. Rollinson, H.R. A terrane interpretation of the Archaean Limpopo Belt. *Geol. Mag.* **1993**, *130*, 755–765. [CrossRef]
28. Valković, V. Radioactive nuclides in nature. In *Radioactivity in the Environment*, 1st ed.; Elsevier: Amsterdam, The Netherlands, 2000.
29. Awad, H.A.; Zakaly, H.M.; Nastavkin, A.V.; El Tohamy, A.M.; El-Taher, A. Radioactive mineralizations on granitic rocks and silica veins on shear zone of El-Missikat area, Central Eastern Desert, Egypt. *Appl. Radiat. Isot.* **2021**, *168*, 109493. [CrossRef]
30. Mohamed, F.H. Rare metal-bearing and barren granites, Eastern Desert of Egypt: Geochemical characterization and metallogenetic aspects. *J. Afr. Earth Sci.* **1993**, *17*, 525–539. [CrossRef]
31. Sabet, A.H. Tin-Tungsten and Rare-Metal Mineralization in the Central Eastern Desert of Egypt. *Ann. Geol. Surv. Egypt* **1973**, *3*, 75–86.
32. Abu El-Leil, I.A. Geology, Petrography and Geochemistry of the Granitid Rocks of Abu Dabbab Area, Eastern Desert. Master's Thesis, 1975.
33. El-Tabal, H.K. Mineralogical Studies on Some Rare Metal Apogranites from Nuweibi and Abu Dabbab Areas, Eastern Desert, Egypt. Master's Thesis, Al-Azhar University, Cairo, Egypt, 1979; pp. 1–112.
34. Sabet, A.H.; Abu El-Leil, I. Geology and Petrography of the Granitic Rocks Along Wadi Abu-Dabbab, Eastern Desert, Egypt. *Ann. Geol. Surv. Egypt* **1985**, *15*, 123–128.
35. Hamimi, Z.; Zoheir, B.A.; Younis, M.H. Polyphase deformation history of the Eastern Desert tectonic terrane in northeastern Africa. In Proceedings of the XII International Conference "New Ideas in Earth Sciences", Moscow, Russia, 8–10 April 2015.
36. Heikal, M.T.S.; Abd, M.; Monsef, E.; Goma, S.R.; Mansi, E.; Top, G. Natural Radionuclides Levels and their Geochemical Characteristics of Abu Dabbab Albite Granite Mining Area, Central Nubian Shield of Egypt. *J. Environ. Hazard.* **2019**, *2*, 10000111.
37. El-Desoky, H.M. Geology, Geochemistry and Genetic Implications of the Greisen Deposits, Central Eastern Desert, Egypt. *Ann. Geol. Surv. Egypt* **2020**, *37*, 128–164.
38. Renno, A. *Zur Petrogenese der Albitgranite von Abu Dabbab und Nuweibi, Central Eastern Desert, Ägypten*; Logos: Berlin, Germany, 1997.
39. Helba, H.; Trumbull, R.B.; Morteani, G.; Khalil, S.O.; Arslan, A. Geochemical and petrographic studies of Ta mineralization in the Nuweibi albite granite complex, Eastern Desert, Egypt. *Miner. Depos.* **1997**, *32*, 164–179. [CrossRef]
40. Sabet, A.H.; Tsogoev, V.B.; Sarin, L.P.; Azazi, S.A.; El Bedewi, M.A.; Ghobrial, G.A. Tin-tantalum deposit of Abu Dabbab. *Ann. Geol. Surv. Egypt* **1976**, *6*, 93–117.
41. Daggett, P.H.; Morgan, P.; Boulos, F.K.; Hennin, S.F.; El-Sherif, A.A.; El-Sayed, A.A.; Basta, N.Z.; Melek, Y.S. Seismicity and active tectonics of the Egyptian Red Sea margin and the northern Red Sea. *Tectonophysics* **1986**, *125*, 313–324. [CrossRef]
42. Pirajno, F.; Cawood, P.A. *Hydrothermal Processes and Mineral Systems*; Springer: Berlin, Germany, 2009.
43. Wilcockson, W.H.; Tyler, W.H. On an area of ultrabasic rocks in the Kassala Province of the Anglo-Egyptian Sudan. *Geol. Mag.* **1933**, *70*, 305–320. [CrossRef]
44. Rittmann, A. On the serial character of igneous rocks, Egypt. *J. Geol.* **1957**, *1*, 23–48.
45. Shukri, N.M.; Lotfi, M. The geology of the Bir Barramiya area. *Bull. Fac. Sci. Cairo Univ.* **1959**, *34*, 83–130.
46. Bogoch, R.; Magaritz, M. Immiscible silicate-carbonate liquids as evidenced from ocellar diabase dykes, southeast Sinai. *Contrib. Miner. Pet.* **1983**, *83*, 227–230. [CrossRef]
47. Streckeisen, A. Plutonic rocks: Classification and nomenclature recommended by the IVGS sub-commission on the systematic of igneous rocks. *Geotims* **1973**, *18*, 26–30.

48. Brown, E.H.; Bradshaw, J.Y.; Mustoe, G.E. Plagiogranite and keratophyre in ophiolite on Fidalgo Island, Washington. *Geol. Soc. Am. Bull.* **1979**, *90*, 493–507. [CrossRef]
49. Sinton, J.M.; Byerly, G.R. Silicic differentiates of abyssal oceanic magmas: Evidence for late-magmatic vapor transport of potassium. *Earth Planet. Sci. Lett.* **1980**, *47*, 423–430. [CrossRef]
50. Barker, F.; Arth, J.G. Generation of trondhjemitic-tonalitic liquids and Archean bimodal trondhjemite-basalt suites. *Geology* **1976**, *4*, 596–600. [CrossRef]
51. Defant, M.J.; Drummond, M.S. Derivation of some modern arc magmas by melting of young subducted lithosphere. *Nature* **1990**, *347*, 662–665. [CrossRef]
52. Botros, N.S. Geological and Geochemical Studies on Some Gold Occurrences in the North Eastern Desert, Egypt. Ph.D. Thesis, Zagazig University, Zagazig, Egypt, 1991; p. 146.
53. Emam, A. Mineralogical and Geochemical Studies on Some Gold Deposits and Host Rocks, Wadi Allaqi, South Eastern Desert, Egypt. Ph.D. Thesis, South Valley University, Hurghada, Egypt, 2005.
54. Torabi, G.; Morishita, T.; Arai, S. Two types of plagiogranite from Mesozoic Ashin ophiolite (Central Iran): A mark of tectonic setting change from Jurassic to Cretaceous. *Geotectonics* **2019**, *53*, 110–124.
55. Hunter, D.R. The role of tonalitic and trondhjemitic rocks in the crustal development of Swaziland and the eastern Transvaal, South Africa. *Dev. Petrol.* **1979**, *6*, 301–322.
56. Hietanen, A. *Idaho Batholith near Pierce and Bungalow, Clearwater County, Idaho*; United States Government Printing Office: Washington, DC, USA, 1963.
57. O'Conner, J.T. A classification of quartz-rich igneous rocks based on feldspar ratios. *US Geol. Surv. Prof. Pap.* **1965**, *82*, 462–465.
58. Hansen, J.; Skjerlie, K.P.; Pedersen, R.B.; De La Rosa, J. Crustal melting in the lower parts of island arcs: An example from the Bremanger Granitoid Complex, west Norwegian Caledonides. *Contrib. Miner. Pet.* **2002**, *143*, 316–335. [CrossRef]
59. Barker, F. Trondhjemite: Definition, environment and hypotheses of origin. In trondhjemites, dacites, and related rocks. *Dev. Petrol.* **1979**, *6*, 651–659.
60. Deer, W.A.; Howie, R.A.; Zussman, J. *An Introduction to the Rock Forming Minerals*; Longman Group Ltd.: London, UK, 1966; 528p.
61. Coleman, R.G.O. *Ophiolites. Ancient Oceanic Lithosphere?* Springer: Berlin/Heidelberg, Germany, 1977.
62. Allègre, C.; Minster, J. Minster, Quantitative models of trace element behavior in magmatic processes. *Earth Planet. Sci. Lett.* **1978**, *38*, 1–25.
63. Harris, N.B.W.; Pearce, J.A.; Tindle, A.G. Geochemical characteristics of collision-zone magmatism. *Geol. Soc.* **1986**, *19*, 67–81.
64. McDonough, W.F.; Sun, S.S. The Composition of the Earth. *Chem. Geol.* **1995**, *120*, 223–253.
65. Sun, S.S.; McDonough, W.F. Chemical and isotopic systematics of oceanic basalts: Implications for mantle composition and processes. *Geol. Soc.* **1989**, *42*, 313–345.
66. Koepke, J.; Berndt, J.; Feig, S.T.; Holtz, F. The formation of SiO_2-rich melts within the deep oceanic crust by hydrous partial melting of gabbros. *Contrib. Miner. Pet.* **2007**, *153*, 67–84.
67. Harris, J.R.; Rencz, A.N.; Ballantyne, B.; Sheridon, C. Mapping altered rocks using LANDSAT TM and lithogeochemical data: Sulphurets-Brucejack Lake district, British Columbia, Canada. *Photogramm. Eng. Remote Sens.* **1998**, *64*, 309–322.
68. Darnely, A.G. Hot granites. Some general remarks in uranium in granites. *Geol. Surv. Can.* **1982**, 23–81.
69. Turekian, K.K.; Wedepohl, K.H. Distribution of the elements in some major units of the earth's crust. *Geol. Soc. Am. Bull.* **1961**, *72*, 175–192.
70. Solovov, A.P.; Dosanova, B.A.; Kosheleva, I.A. Analysis of results of lithochemical exploration in metallo-genic-prospecting. *Int. Geol. Rev.* **1971**, *13*, 954–965.
71. Wakabayashi, J.; Dilek, Y.; Moores, E.M.; Elthon, D.; Nicolas, A. Spatial and temporal relationships between ophiolites and their metamorphic soles: A test of models of forearc ophiolite genesis. In *Phiolites and Oceanic Crust: New Insights from Field Studies and the Ocean Drilling Program*; Geological Society of America: Boulder, CO, USA, 2000; pp. 53–64.
72. Cox, J.; Searle, M.; Pedersen, R. The petrogenesis of leucogranitic dykes intruding the northern Semail ophiolite, United Arab Emirates: Field relationships, geochemistry and Sr/Nd isotope systematics. *Contrib. Miner. Pet.* **1999**, *137*, 267–287.